Temporal Processing in Primate Motor Control: Relation Between Cortical and EMG Activity

Olivier F. L. Manette and Marc A. Maier

***Abstract*—We investigated spatio-temporal information processing in the primate motor system. Corticomotoneuronal (CM) cells provide monosynaptic excitatory connections from motor cortex to spinal motoneurons and contribute causally to the time-varying electromyogram (EMG) of their target muscle. A multilayer perceptron (MLP) was used to evaluate the transfer function between neural activity of single CM cells and their target muscle EMG, using data from in-vivo recordings in primate motor cortex. For an optimal MLP performance, i.e., minimal error between recorded target EMG and MLP-derived EMG, the CM cell input period had to span the latency observed between CM cell peak activity and EMG peak activity. We argue that the same spike train may code two types of information: 1) rate coding within the input window accounted for large-amplitude variations in the EMG signal and 2) temporal coding within a window of 40 ms just prior to the EMG output signal accounted for EMG variations of small amplitude. The transfer function of the MLP, thus, combines rate and temporal coding and suggests that CM cell output may also combine these two forms of coding. We predict that mutual constraints of rate and temporal coding would, however, would limit the CM output to code for particular temporal profiles of EMG, possibly adapted to bio-mechanical constraints.**

***Index Terms*—Backpropagation, biological motor system, biological system modeling, brain modeling, electromyography, neural network applications, perceptron, transfer function.**

I. Introduction

BIOLOGICAL skeleto-motor control contracts muscles through the activation of spinal motoneurons, the final common pathway. The output of the ensemble (pool) of motoneurons activating a given muscle can be quantified by measuring the electromyogram (EMG). The input to the motoneurons is more difficult to establish. Many cells in diverse cortical motor areas have been shown to code (through rate-coding) *high-level* movement parameters such as force [1], direction [2], amplitude or velocity [3]. Indeed, some cortical cells have been shown to code for several of those parameters [4]. On the other hand, phenomena on time scales akin to temporal coding have been described: on the cortical level, occurrence of synchrony has been shown in several cortical areas [5] and also among motor cortical cells [6]. At a *low* level of motor control, i.e., at the level of muscles and motoneurons, it was shown that motoneurons among the same pool tend to be synchronyzed [7] in the ms range and even motoneurons of different muscles show synchrony, though to a smaller degree [8].

How these high-level cortical codes in the frequency and temporal domain are related to low-level muscle activation is less well understood. One of the problems is, that the output connectivity of those cortical cells is often unknown. However, progress has been made by characterizing the activity and connectivity of neurons projecting directly to motoneurons (so-called premotor neurons). In the following, we will briefly document their properties.

A. Effects of CM Spikes in the Frequency Domain

In the monkey, several neuronal populations contribute to the activation of the motoneurons [9], [10] and, hence, to EMG activity. However, because these sources converge onto the same motoneurons, the various contributions of cannot be differentiated in the output EMG. Among the premotor populations are the corticomotoneuronal (CM) cells with direct, monosynaptic and excitatory connections from the motor cortex to spinal motoneurons [11], [12]. For CM cells, rate-coding with respect to movement parameters has been investigated: some of them show correlations between firing-rate and force [13], [14]. However, a pertinent question for CM cells is, what is their relation to *low-level* control such a muscle activity. The activation patterns of CM cells within a colony projecting to the same target muscle vary: for a tonically activated muscle, the input profile of CM cells is predominantly tonic, phasic-tonic, or phasic [13]. However, it is not clear how these temporal patterns influence the pattern of the target EMG.

Some CM cells also show correlations between firing-rate and target EMG activity [14]. The temporal relations in the frequency domain are more variable and at a range of hundreds of ms in contrast to the precise timing based on conduction velocity (in the ms range). Onset time for most CM cells is in the order of -200–100 ms around the target muscle EMG onset. The majority of CM cells are activated prior to target muscle EMG, with an average latency of around -70 ms [13].

B. Effects of CM Spikes in the Range of the Conduction Delay

Measures in the domain of temporal coding, such as cortico-muscular coherence in humans and in the monkey, indicate that cortical synchrony affects the EMG [15], [16]. In a similar time frame, postspike effects of full-wave rectified EMG (absolute value of the raw EMG), revealed by spike-triggered averaging (STA), provided clear evidence that populations of CM cells activate a given target muscle through their monosynaptic

Manuscript received May 30, 2003; revised December 19, 2003. This work was supported in part by a European Fifth Framework Programme Grant IST-2001-33073, in part by Institut National de la Santé et de la Recherche Médicale (INSERM), and in part by French Grant ACI Neurosciences Intégratives et Computationnelles 02 2 0667

The authors are with the INSERM U483, Université Pierre et Marie Curie, 75005 Paris, France (e-mail: Marc.Maier@snv.jussieu.fr).

Digital Object Identifier 10.1109/TNN.2004.833127

connections to motoneurons. A postspike facilitation (PSF) i.e., a small and temporary increase in EMG activity time-linked to the triggering spikes of the triggering CM cell, is characteristic for premotor neurons. The cortico-muscular conduction delay (delay between the emission of the cortical spike and the onset of the PSF in the EMG) for hand muscles, as measured by STA, is in the order of 5 ms (for forearm muscles) to 16 ms (for intrinsic hand muscles), consistent with an excitatory, monosynaptic pathway [11], [12]. The PSF is a short temporal phenomenon (less than 30 ms) and its amplitude, measured by the MPI (mean percent increase of the postspike facilitation), depends on several variables (such as the background EMG activity) and provides only an indirect measure of synaptic strength [17].

Whereas variations in CM cell firing will be reflected in the EMG with a delay in the order of a few ms, these same variations in the frequency domain, as judged by the CM cell onset latency, will affect the EMG with a delay of about 100 ms. How can those two effects be combined?

C. Open Questions and Neural Network Approach for a Tentative Answer

We used an artificial neural network approach in conjunction with biological input–output data to tentatively provide answers to the following questions:

1) what is the correlation between the temporal profile of CM cell activity and the profile of overall EMG activity? As briefly described in Sections I-A and B, evidence for rate- as well as temporal coding has been established. We attempt to answer through a method that does not include an *a-priori* hypothesis on the code;

2) what type of transfer function exists between CM cell input to motoneurons and EMG output activity? Several attempts have been made to characterize the transfer function between motoneuron input and output [18] as well as between motoneuron-activity and EMG, e.g., [19]. We aim at finding characterizing the relation between CM cell and EMG activity by ignoring the motoneuronal transform;

3) is a particular period in the CM cell spike train of significant importance for the input–output relation? This relates to the previous two questions: if rate- and temporal coding were convolved or multiplexed, we would expect to find periods of the spike train with varying importance with respect to those two codes;

4) is there a relation between the size of the experimentally observed PSF and the performance of the perceptron? This more technical question will be taken up below.

A perceptron was used to evaluate the transfer function between CM cell activity and target muscle EMG, e.g., [20]. The choice of the perceptron was motivated by several factors, which are: 1) the perceptron does not rely on underlying assumptions on the existence of rate coding or temporal coding; 2) it allows the use of the raw input signal without making assumptions on prior treatment or extraction of variables; 3) the perceptron, rather than a recurrent architecture, was chosen because of the similarity to the forward connectivity between CM cell and motoneuron; and 4) after learning, the perceptron incorporates an implicit transfer function even if there is only a partial input–output relation, and its performance indicates the degree to which the input predicts the output.

This approach takes a simplified view and treats the CM system, in a first approximation, as a simple input–output system: the input is provided by the CM cell spike train, the output by the EMG and the MLP provides the transfer function, implemented on the biological level by the motoneurons or the spinal network. This simplification neglects other sources of input, but even then, already within this single system questions about its spatio-temporal information processing arise and need to be answered. We tried to dissociate the influence of other premotoneuronal sources in the MLP transfer function by taking into account the full CM cell spike train and its target muscle EMG independent of behavioral epochs. This was done in order to maximize the variance in the CM-EMG relation, so as to minimize the covariation between the CM input and unknown inputs from other sources [21].

II. Method

We used an artificial neural network approach to explore the above issues and to evaluate the transfer function between the temporal CM cell activity (at the single cell level) and its target muscle EMG.

A. Experimental Data

The biological data consisted of recordings from CM cell activity in primate motor cortex identified by the presence of PSF in their respective target EMG obtained by STA. Data were obtained from one monkey (macaca mulatta) and for 19 CM cells during a precision grip task that required the use of the index finger and thumb to move two spring-loaded levers into a target position and hold them there for 1 s. For the selected CM cells, peak activity arose prior to or at peak target EMG activity. Data were sampled for periods of at least 120 s, with a sampling rate of 5 kHz [6]. The EMG was full-wave rectified and smoothed with a 10 ms or a 40 ms sliding window. PSTH of CM cell activity as well as averaged EMG activity was compiled for up to 100 trials, aligned on the force onset of correct trials (see Fig. 1). Peak-to-peak latency from the PSTH and averaged EMG was used to quantify the latency between CM cell and EMG activity.

B. Multilayer Perceptron: Input and Output

The input–output function between CM cell activity and EMG was modeled by a fully connected multilayer perceptron (MLP under MATLAB) with a single output unit, a single hidden layer with 2–25 hidden units, and a varying size of input units (10–200). The input vector consisted of a binary sequence corresponding to spikes of the CM cell over a given period Δ (Fig. 1), which corresponded to a window of varying size into the past of the CM cell activity (down-sampled to 4 ms bin size). Each input unit received a binary input corresponding to the presence or absence of a spike in its bin, i.e., there were as many input units as bins. The output unit was supposed to code the target muscle EMG amplitude (a positive scalar) at time t, given by the recorded EMG amplitude, with Δ prior to t. Input and output data for learning were selected so as to represent the

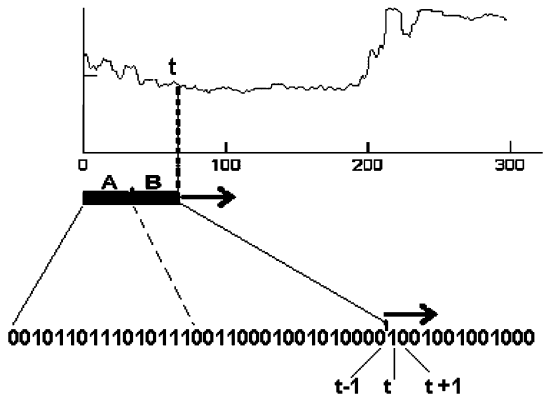

Fig. 1. Use of MLP. Input: binary CM cell activity over interval of time Δ (1 indicates presence, 0 absence of a spike within a bin of 4 ms). Output: EMG activity at the instant t. In this example, the input window Δ is positioned between $t-\Delta$ and $t-1$. The interval can be divided into (a) long-term period and (b) short-term period.

maximally observed variance in the output (EMG). First, intertrial activity as well as activity corresponding to correct and false trials was used. Second, all observed levels of EMG were treated equally, independent of their actual distribution during a recording session, i.e., the same number of examples were used for predicting each value of EMG. Thus, after learning, the MLP provided an implicit transfer function (prediction) for the EMG amplitude at time t, based on the CM cell activity in the period Δ.

C. Multilayer Perceptron: Parameters

Input layer units and the output unit used the identity function and hidden layer units a sigmoidal activation function. The optimal size of the hidden layer was determined by minimizing the size of the hidden layer in relation to the error and was kept constant (15 units). Learning was achieved by providing inputs and corresponding outputs for a period of 120 s of data, using backpropagation (batch gradient descent). The number of learning iterations was determined by "early stopping." 100 random initializations (Nguyen-Widrow) were used for each MLP and the best solution kept.

D. Multilayer Perceptron: Transfer Function and Performance Criterion

The transfer function $gi(\mathrm{CM}i\,[t-\alpha, t-\beta], w) = Si(t)$ relates an interval $\Delta = \beta - \alpha$ of activity of CM cell i to its target muscle EMGi activity at t via weights w. $Si(t)$ should tend toward EMG$i(t)$. The interval Δ was either continuous with the bin at t, or there was a gap of β bins between the Δ and t.

The error E was normalized with respect to the maximal error $E_{\max}$, which consisted of an MLP output corresponding to the mean EMG activity produced by the bias units. Performance P was calculated as $P = 1 - (E/E\max)$ with $\mathrm{E}\max(\mathrm{t}) = \sum_{\mathrm{t=1}}^{N}(\mathrm{EMG(t)/N}) - \mathrm{EMG(t)})$, for a period of N bins in the EMG.

E. MLP-Mediated Postspike Effects

After learning, a procedure equivalent to STA was used to calculate MLP-mediated postspike effects. The MLP output was calculated for a period of 104 ms (26 bins) centered around each triggering spike occurring at bin 13 and then averaged across spikes. Spikes surrounding the triggering spike within the 104 ms interval were taken into account and contributed to the nontriggered output, corresponding to the background EMG activity in STA. Postspike facilitation (onset, amplitude, surface) was characterized with respect to the pretrigger baseline taken as the maximal output during pretrigger period.

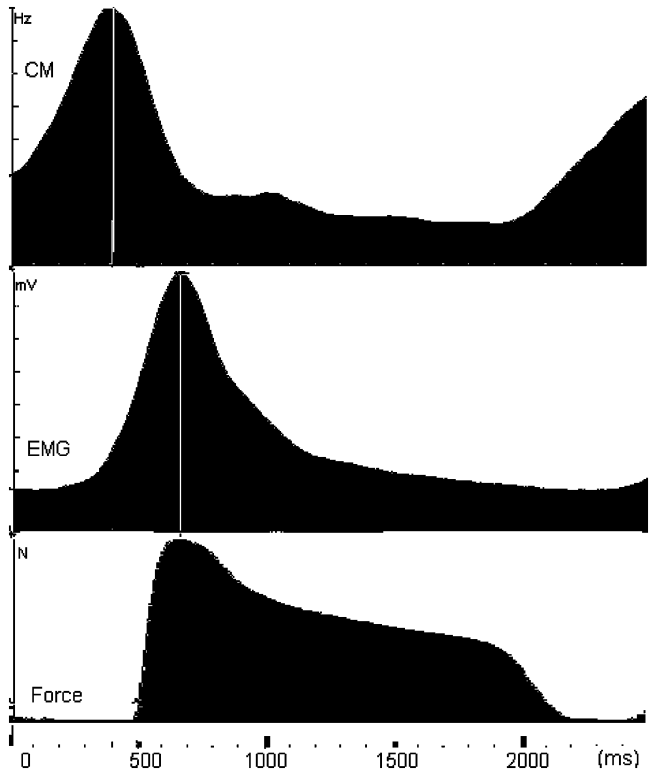

Fig. 2. Example of experimentally obtained data during a precision grip paradigm. Top: PSTH of CM cell activity over 100 trials Middle: corresponding average rectified EMG of the target muscle (abductor pollicis brevis). Bottom: corresponding average force exerted by the index finger. The three recordings were carried out simultaneously and aligned on force onset. Peak CM cell activity precedes peak EMG by 300 ms.

III. Results

Fig. 2 shows an example of the biological data: PSTH of CM cell activity and averaged rectified EMG activity of the target muscle are aligned on force onset. In this case, the peak-to-peak delay between the phasic-tonic CM cell and EMG activity was 300 ms; the conduction delay, as judged by the PSF (not shown) was 14 ms.

A. MLP Performance

The performance of the MLP in predicting the EMG amplitude at t varied as a function of the *size* of the input window, i.e., with the size of the period of CM activity Δ prior to t. Fig. 3 shows the MLP performance curves for 6 CM cells after learning over at most 50 iterations (early stopping). For each cell, only the best performance curve is shown, selected from a pool of 100 different random initializations per data point. The window size varied from 40–520 ms in steps of 40 ms.

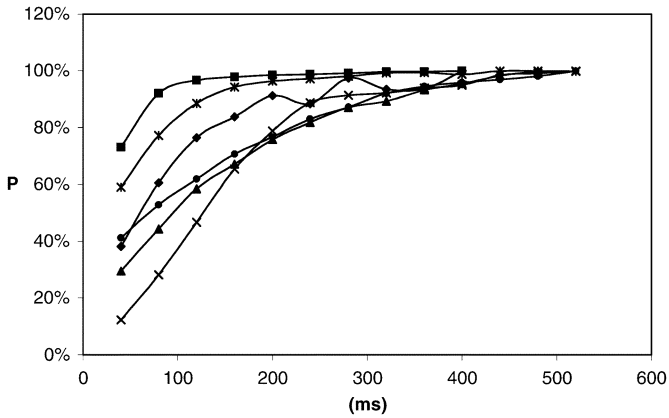

Fig. 3. MLP performance as a function of the size of the input window for 6-CM cells. One trace per cell. For each of the 13 data points per cell, the input window was incremented by 40 ms. This corresponds to an increasing window size from 40–520 ms. For each data point, MLPs were trained based on 100 random initializations and maximal performance is plotted.

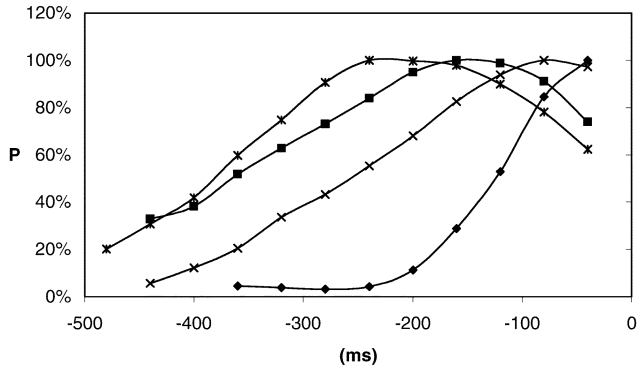

Fig. 4. MLP performance as a function of the position of the input window for four cells. A window of fixed size (80 ms) is shifted into the past (away from t) by 40 ms. Peak performance is achieved around the CM cell-EMG peak-to-peak latency (-40 ms, –80 ms, –160 ms, and –240 ms).

Increasingly larger input windows increased the MLP performance and optimum is reached between 40–320 ms, i.e., at a input window size that covers the peak-to-peak latency between CM cell and EMG activity. At intervals longer than this latency the performance saturated. Maximal overall performance varied from 16% to 31% for the 162 CM cell-EMG pairs tested.

We then tested whether the MLP could predict the EMG with a small window of constant size. We determined the optimal window *position* by sliding an input window of constant size $(\Delta = 80 \text{ ms})$ over a period from 4 to 320 ms prior to t (increasing α and $\beta = \alpha - 80$). Fig. 4 shows the MLP performance curve as a function of window position for four different cells. Depending on the cell, the performance curve varied in terms of shape and peak location. For the first cell, the MLP had a peak performance with a window centered on -40 ms and performance decreased with increasing gaps (β) between the window and t. For the other two three cells the peaks occurred for windows centered on –80, –160, and –240 ms, respectively.

Over the populations of 16 cells tested, the window position for maximal performance was in direct relation with the peak-to-peak latency between CM cell and EMG target activity, as shown in Fig. 5. Furthermore, for all cells the maximal performance with the constant-sized input window of 80 ms was smaller than that obtained with a contiguous window.

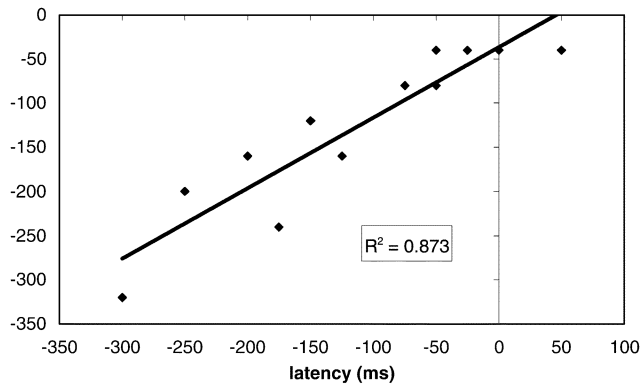

Fig. 5. Scatter plot between optimal position of the input window (in bins) and the CM cell-EMG peak-to-peak latency. A significant positive correlation was obtained ($R^2 = 0.837$, $N = 16$, four points overlapped) is obtained.

B. MLP-Mediated Postspike Effects and Biological Postspikes Effects

Since all tested CM cells by definition had a postspike effect, we wanted to verify whether the best solution found by the MLP also created a PSF-like effect. We also characterized the possible influence of the spike train on the PSF. We applied two types of spike trains that differed with respect to the spikes in the vicinity $(\pm 50 \text{ ms})$ of the triggering spike, which are: 1) no activity at all except for the triggering spike, and 2) the recorded input, i.e., taking into account spikes prior to or after the triggering spike. Fig. 6 shows the MLP output for ± 50 ms around the triggering spike. In the first case, without firing history being taken into account, a clear PSF-like effect appears [Fig. 6(a)] with an onset at 12 ms (three bins). In addition, in the second case where firing history was accounted for [Fig. 6(b)], a PSF-like increase can also be seen, though with a different shape and an onset at 16 ms (four bins).

We quantified this PSF-like effect of the full spike train by measuring its amplitude normalized to the pretrigger baseline. Fig. 7 shows the positive correlation between the size (MPI) of the biological PSF and the amplitude of the MLP-mediated postspike effect.

We then wanted to verify whether the size of the biological postspike effect (MPI) was related to the performance of the MLP. Overall performance of the MLP, varying between 6%–31%, was not related to biologically measured MPI: there was no significant correlation between these two measures ($N = 12$, $R^2 = 0.02$).

C. Differential Importance of Spikes Within the Input Window

To investigate the importance of spikes within the input window, we divided the input window, with Δ covering the latency estimated by the performance curve (Fig. 4), into two periods. A first period $[t - \Delta, t - \Delta/2]$ referred to as "long-term" period [Fig. 1(a)] because situated a long time from t. A second period, covering $[t - \Delta/2, t - 1]$ contiguous with t and the first period, referred to as "short-term" period [Fig. 1(b)].

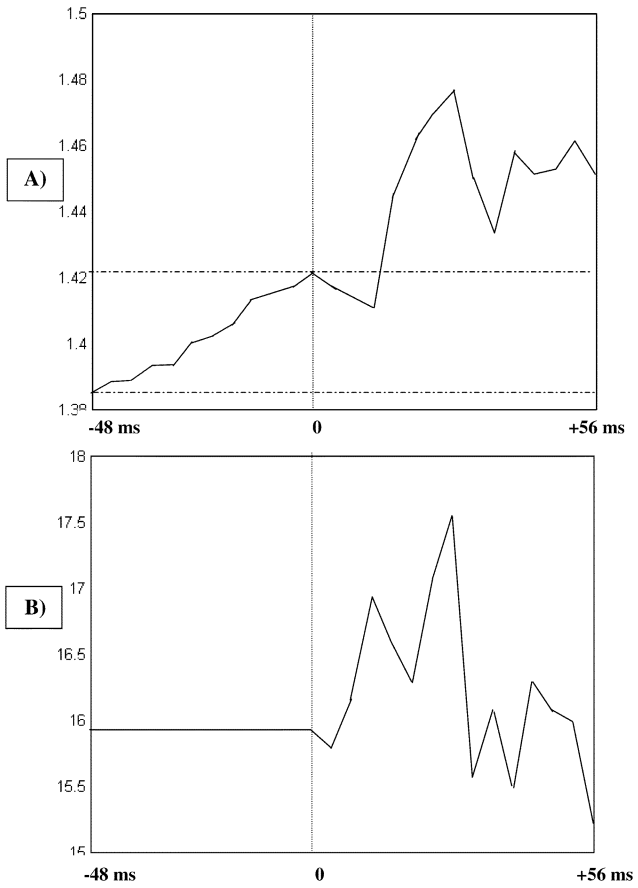

Fig. 6. MLP-mediated postspike effects. Example from one MLP over a period of ± 50 ms (26 bins) around the triggering spike (stippled vertical line). (a) Postspike effect with real, experimentally recorded spike train (history). Stippled vertical lines indicate minimal and maximal amplitude in the pretrigger period. (b) Postspike effect of the same MLP without preceding or following spikes (no history of the spike train).

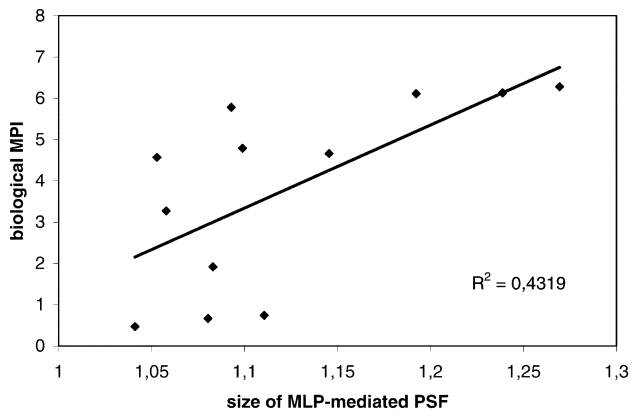

Fig. 7. Size of the biologically recorded postspike effect (MPI) as a function of the amplitude of the MLP-mediated postspike effect. Significant positive correlation: $R^2 = 0.43$, $N = 12$ cells.

After learning based on activity within both periods, MLP output was simulated for the following three different conditions: 1) with spikes in the long- and short-term period as used during learning; 2) with spikes in the long-term period only; and 3) with spikes in the short-term period only. Fig. 8(a)–(c) shows an example of MLP output over 4 s for these three cases, superimposed with the real target EMG. There were qualitative

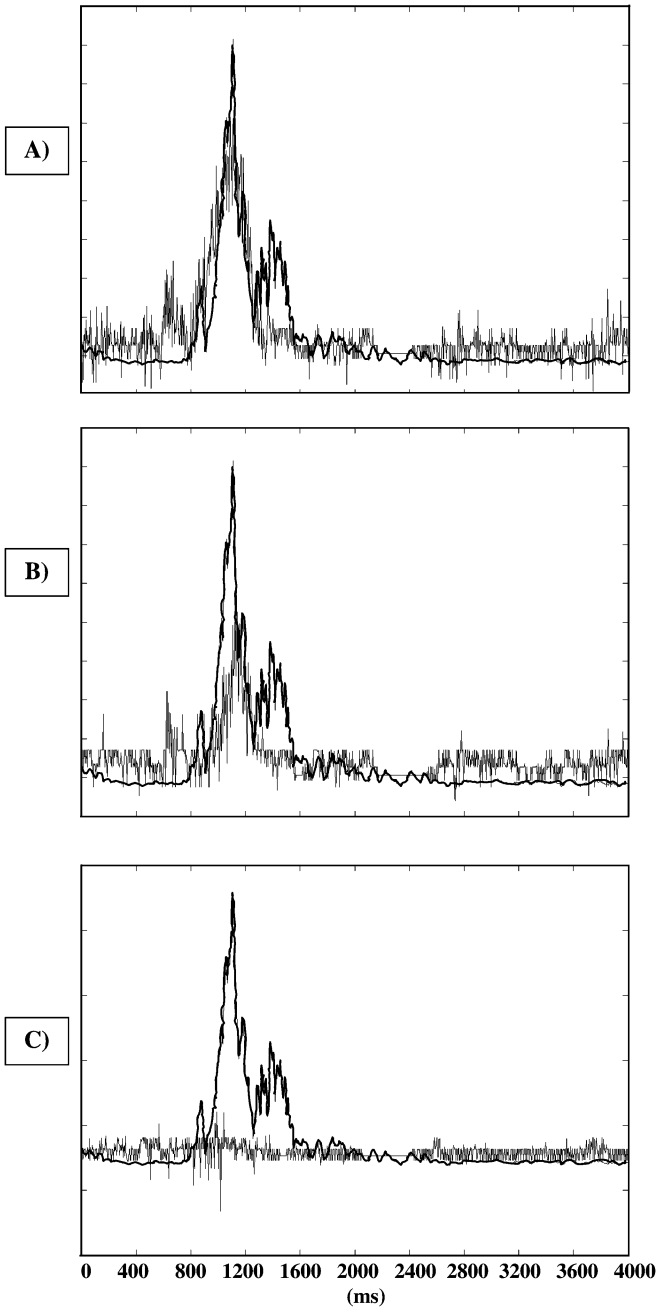

Fig. 8. Importance of early (short-term period) versus late half (long-term period) of data within the input window. (a) MLP performance with long- and short-term data. Recorded EMG (thick trace) versus calculated EMG (thin trace) over 4 s for a single MLP. (b) MLP performance with long-term data only over the same period as in (a). Compared to (a) performance decreases qualitatively. (c) MLP performance of short-term data only: they only code for small variations.

differences in the MLP output indicating a differential contribution of spikes belonging to those two periods. The best fit between MLP output and real EMG was achieved with the use of both periods [performance $P = 40\%$, Fig. 8(a)]. Using spikes in the long-term period only produced a qualitatively lower performance but the output still followed the global variations of the EMG. However, the use of only short-term spikes prevented the MLP output from following the global variations: the output varied to a small degree around the constant averaged EMG activity.

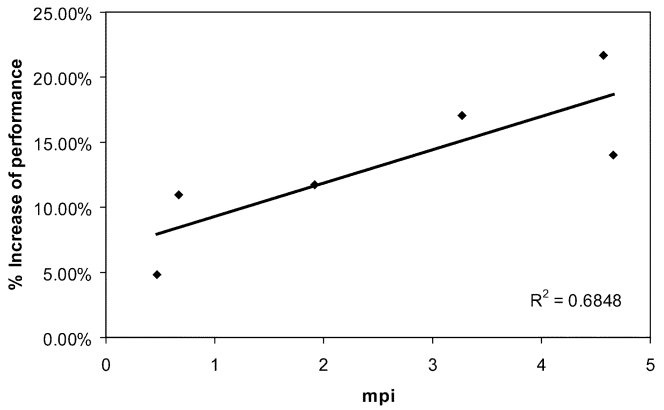

Fig. 9. Improvement of MLP performance when short-term data were included during learning over that of learning with long-term data only. The degree of improvement is correlates positively with the size of the biological postspike effect ($R^2 = 0.68$, $N = 6$ cells). The positive correlation indicates that the importance of the short-term data increases with the size of the postspike effect.

Thus, on a first view, the short-term period, by only varying around the mean activity, did not seem to be able to improve performance of the MLP. To check whether the short-term period could quantitatively contribute to overall performance and how, we selected within the short-term period a window of 40 ms prior to t that potentially contributes to the postspike effect. In addition, within the long-term period we chose a 80 ms window centered on the latency for the peak performance (Fig. 4). Thus, we used a fixed-size long-term window and a noncontiguous fixed-size short-term window. This was done for 6 cells where it was possible to clearly define a nonoverlapping long- and short-term period. In order to quantify the gain in performance due to spikes within the short-term period we tested two conditions of learning, which are: 1) based on spikes within those two periods and 2) based on spikes in the long-term period only. We found that the combination of the two periods improved the performance in all six MLPs by 14% on average over that seen after having learned with the long-term spikes only ($SD = 5.7\%$). Thus, the MLP did indeed use short-term information contained within a window of 40 ms prior to t to improve its performance. Finally, we checked whether the degree of the improvement depended on the size of the postspike effect. This was the case: Fig. 9 shows the positive correlation ($N = 6$, $R^2 = 0.68$) between the increase in performance and the size of the experimentally determined postspike effect (MPI).

IV. Discussion

We wanted to investigate what kind of code CM cells use to control EMG activity. CM cells are causally involved in producing EMG activity via their monosynaptic excitatory connections to motoneurons in the spinal cord. We have used a computational approach based on a multilayer perceptron (MLP) in order to predict the target muscle activity at time t as a function of CM single cell input over an interval Δ prior to t. We will in the following address the basic questions put forward in the introduction.

A. Overall Input–Output Relation

A first question concerned the relation (degree of correlation) between single CM cell activity and EMG activity. The MLP approximates the best possible contribution of a single cell. By using multiple randomizations and choosing the best one we tried to estimate the maximal contribution in terms of MLP performance. The performance was between 16%–31%. Clearly, a single CM cell determines the EMG output only partially. But this performance seems rather high considering that a single CM cell is one among a colony of CM cells projecting to the same target muscle and that CM cells typically branch to more than one target muscle.

B. Rate Coding

The MLP data suggest that a large part of the input–output relation can be explained by rate coding. Spikes falling within an optimal window centered around the latency between CM cell peak and EMG peak activity can code for the global variations in the target EMG. This is in keeping with biological data that CM cell firing frequency can be correlated with target EMG activity [14]. However, rate coding does not seem to contain sufficient information to produce finer variations in the EMG.

The results further suggest that rate coding over a window provides better MLP performance than instantaneous rate coding. On the biological level, it has been shown that motoneurons, with limited dynamics in firing rate modulation, may act as a low-pass filter [22] partly due to long after-hyperpolarization [23]. Furthermore, it was estimated that the temporal population output of a CM cell colony was more phasic than its target muscle EMG activity [9]. Thus, on the level of information processing, rate coding over a sufficiently large window of input spikes, which also acts as a low-pass filter, improves the transfer function. This is compatible with the finding that MLP performance increased with increasing size of the input window: the optimal size of the window was in the order of the CM cell-EMG peak-to-peak latency, i.e., up to 300 ms. However, smaller windows (80 ms) centered on this latency also allowed for efficient rate coding, indicating that spikes in particular periods may contain more information than in others.

C. Temporal Coding

The results of the MLP analysis suggest that CM cell activity in terms of a transfer function for EMG activity also contains information in the temporal domain. In particular, the transfer function learned by the MLP also produced effects akin to those of biological postspike facilitation (PSF) of EMG activity by CM cells [11], [12]. These MLP-mediated postspike effects were specific for spikes occurring within bins (input units) close to time t, i.e., corresponded to direct effects mediated by the conduction delay. Furthermore, we found that the size of the MLP-mediated PSF was related to the size of the biological PSF, indicating that the MLP in terms of information processing may have captured a similar relation. Of course, there is no mechanistic relation between the biological PSFs produced via EPSPs in motoneurons and that used by the MLP. Importantly, however, short-term information in the range of the conduction delay did significantly contribute to the MLP performance. In particular, small variations in the EMG were captured by spikes in the short-term range and not in the domain of rate coding.

On the biological level, mechanisms akin to temporal coding have been described at the motoneuronal level and in the corticospinal system: motoneurons among the same [7] or different pools tend to be synchronyzed [8] on the cortical level, synchrony has been described among motor cortical cells [e.g., [6]] and also between CM cells [24], [25].

D. Formal Level—Combination of Rate and Temporal Coding

On a formal level, the MLP transforms a binary coded input sequence within a temporal window into a real-valued output occurring as a consequence just after the end of the input window. By subdividing the window into a period containing long-term and another containing short-term spikes, we tried to argue that the long-term part essentially works on rate and the short-term part on temporal coding. For rate coding, the argument relies on the finding that there is a relation between the CM cell, EMG peak-to-peak latency and the window position. For occurrence of temporal coding, the argument is based on the observations that single spikes do indeed contain information since: 1) the MLP-mediated postspike effect correlated with the biologic MPI; 2) a PSF was shown after a single spike; and 3) the MLP performance increased with the addition of short-term spikes. In short, we may consider that there is a tradeoff between rate and temporal coding. However, we do not contend that long- and short-term information are mutually exclusive: it was convenient to highlight them in separate periods, but rate coding is not limited to the long-term period, whereas temporal coding probably is.

Based on our results, we may assume that rate coding determines the gross levels of EMG, whereas, in a complementary fashion, temporal coding provides precision to the EMG. Our data indicate that improvement in MLP performance was correlated to the experimentally assessed size of the PSF. A model for how CM cells code EMG activity may, thus, be as follows: the amplitude or range of EMG activity would be subdivided into several gross levels. CM cell rate code would determine what one of those gross levels. Then, to reach the desired EMG value, temporal coding, i.e., information contained within the last spikes of the train, would adjust the EMG by adding to this gross level. The biological MPI may therefore indicate the average shift from the gross level to the desired EMG provided by the CM cell. Also, it may be indicative of the number of gross levels coded in the frequency domain: the larger the MPI the bigger would be the difference between gross EMG levels (i.e., less levels are coded for in the frequency domain). This may account for the fact, that when short-term information is neglected in MLPs for CM neurons with large MPIs, a larger proportion of information is lost compared to MLPs for CM cells with a small MPI (Fig. 9). This suggests that the MPI may be indicative of the information content in the frequency domain of the CM cell (through an inverse relation).

In summary, a model for the information transmission between CM cell and EMG activity compatible with the MLP results would need to combine rate and temporal coding. The long-term period would indicate the gross level of EMG through rate coding: a linear transfer function would be sufficient and precise spike timing of minor importance. In the short-term period, temporal coding through postspike facilitation, would code for small EMG variations on top of the gross ones. Its transfer function could be based on coefficients attributed to each bin. The total output would then correspond to the sum (superposition) of the two. We suppose that the superposition function could be additive, since we found a linear relation between MPI and increase in MLP performance. The EMG would be coded by: $\mathrm{EMG}(t) = \left(A \sum_{i=t-\alpha}^{t-\beta} bi\right) + \left(\sum_{i=t-k}^{t-1} bi\theta i\right)$, where bi represents the binary value of bin i, the first sum expresses the frequency multiplied by A, a linear function, and the second sum represents temporal coding based on weights θi attributed to each bin i within the short-term window of size $k-1$.

The consequences of such a model are two-fold. First, the number of gross EMG states would be determined by the states available in the CM cell frequency domain. In information theory, the Nyquist equation: $H = n \log_2 V$ determines the quantity of information H (in bits) as a function of n (the number of elements of the message) and V (the number of states in each element). Because, additional information would be contained in the short-term period, the total information content of CM cell activity would be the product of the two. Such a model would provide a parsimonious solution because it allows for the coding of a many-valued output with a limited bandwidth of inputs in the frequency domain.

Second, this kind of coding has consequences in terms of transitions. Information is contained within a temporal window that requires a minimal necessary size Δ to code information. Together with the maximal firing rate F, this window determines the number of possible spike train combinations within Δ, i.e., $2^{\Delta * F}$. This number corresponds to the theoretical maximal number of EMG values the cell can code. However, if part of the window uses rate coding, i.e., average frequency of the spike train, this number will be much lower. Thus, to pass from a given spike train to another train, fully independent of the first, takes at least a time of Δ. Furthermore, to transmit sequences of messages takes proportionally longer and not all kinds of transitions will be feasible due to the size of the window. We would predict that CM cells would be limited to the production of a given set of profiles of output activity: i) because transitions cannot occur arbitrarily fast and ii) because precise sequences would produce particular temporal profiles. This in a wider sense would lead to a specialization of CM cells for particular movements [26]. This specialization of CM cells may be in relation to bio-mechanic limitations: the space of movements is limited and this may in turn limit the number of sensible firing transitions in CM cells. Graph theory [27] may provide a tool for describing the possible transition states of CM cells.

How would the system calculate the coefficients for each bin in the temporal domain? We suggest that this may be done through learning. Two limitations would need to be taken into account: coefficients of neighboring bins cannot be independent and the functions should be compatible with the biology of the neuron.

ACKNOWLEDGMENT

The authors would like to thank S.N. Baker and R.N. Lemon for providing the experimental data (Sobell Department of

Motor Neuroscience and Movement Disorders, Institute of Neurology, UCL, London, U.K.).

REFERENCES

[1] E. V. Evarts, "Relation of pyramidal tract activity to force exerted during voluntary movement," *J. Neurophysiol.*, vol. 31, no. 1, pp. 14–27, 1968.

[2] A. Georgopoulos, J. Kalaska, R. Caminiti, and J. Massey, "On the relations between the direction of two-dimensional arm movements and cell discharge in primate motor cortex," *J. Neurosci.*, vol. 2, pp. 1527–1537, 1982.

[3] D. W. Moran and A. B. Schwartz, "Motor cortical representation of speed and direction during reaching," *J. Neurophysiol.*, vol. 82, pp. 2676–2692, 1999.

[4] Q. G. Fu, D. Flament, J. D. Coltz, and T. J. Ebner, "Temporal encoding of movement kinematics in the discharge of primate primary motor and premotor neurons," *J. Neurophysiol.*, vol. 73, no. 2, pp. 836–854, 1995.

[5] W. Singer and C. M. Gray, "Visual feature integration and the temporal correlation hypothesis," *Ann. Rev. Neurosci.*, vol. 18, pp. 555–86, 1995.

[6] S. N. Baker, R. Spinks, A. Jackson, and R. N. Lemon, "Synchronization in monkey motor cortex during a precision grip task. I. Task-dependent modulation in single-unit synchrony," *J. Neurophysiol.*, vol. 85, pp. 869–885, 2001.

[7] A. K. Datta, S. F. Farmer, and J. A. Stephens, "Central nervous pathways underlying synchronization of human motor unit firing studied during voluntary contractions," *J. Physiol.*, vol. 432, pp. 401–425, 1991.

[8] F. D. Bremner, J. R. Baker, and J. A. Stephens, "Variation in the degree of synchronization exhibited by motor units lying in different finger muscles in man," *J. Physiol.*, vol. 432, pp. 381–99, 1991.

[9] E. E. Fetz, P. D. Cheney, K. Mewes, and S. Palmer, "Control of forelimb muscle activity by populations of corticomotoneuronal and rubromotoneuronal cells," *Prog. Brain Res.*, vol. 80, pp. 437–448, 1989.

[10] E. E. Fetz, S. I. Perlmutter, M. A. Maier, D. Flament, and P. A. Fortier, "Response patterns and postspike effects of premotor neurons in cervical spinal cord of behaving monkeys," *Can. J. Physiol. Pharmacol.*, vol. 74, no. 4, pp. 531–546, 1996.

[11] E. E. Fetz and P. D. Cheney, "Post-spike facilitation of forelimb muscle activity by primate corticomotoneuronal cells," *J. Neurophysiol.*, vol. 44, pp. 751–772, 1980.

[12] R. N. Lemon, G. W. Mantel, and R. B. Muir, "Corticospinal facilitation of hand muscles during voluntary movement in the concious monkey," *J. Physiol.*, vol. 381, pp. 497–527, 1986.

[13] P. D. Cheney and E. E. Fetz, "Functional classes of primate corticomotoneural cells and their relation to active force," *J. Neurophysiol.*, vol. 44, pp. 773–791, 1980.

[14] M. A. Maier, K. M. Bennett, M. C. Hepp-Reymond, and R. N. Lemon, "Contribution of the monkey corticomotoneuronal system to the control of force in precision grip," *J. Neurophysiol.*, vol. 69, pp. 772–785, 1993.

[15] J. M. Kilner, S. N. Baker, S. Salenius, R. Hari, and R. N. Lemon, "Human cortical muscle coherence is directly related to specific motor parameters," *J. Neurosci.*, vol. 20, no. 23, pp. 8838–8845, 2000.

[16] S. N. Baker, E. Olivier, and R. N. Lemon, "Task-dependent coherent oscillations recorded in monkey motor cortex and hand muscle EMG," *J. Physiol.*, vol. 501, pp. 225–241, 1997.

[17] R. Porter and R. N. Lemon, *Corticospinal Function and Voluntary Movement*. Oxford, U.K.: Oxford Univ. Press, 1993.

[18] R. K. Powers and M. D. Binder, "Input–output functions of mammalian motoneurons," *Rev. Physiol. Biochem. Pharmacol.*, vol. 143, pp. 137–263, 2001.

[19] J. A. Hoffer, N. Sugano, G. E. Loeb, W. B. Marks, M. J. O_Donovan, and C. A. Pratt, "Cat hindlimb motoneurons during locomotion. II. Normal activity patterns," *J. Neurophysiol.*, vol. 57, no. 2, pp. 530–553, 1987.

[20] T. Nagai, T. Yamamoto, H. Katayama, M. Adachi, and K. Aihara, "A novel method to analyze response patterns of taste neurons by artificial neural networks," *Neuroreport*, vol. 3, no. 9, pp. 745–748, 1992.

[21] T. Hastie, R. Tibchiriani, and F. Friedman, *The Elements of Statistical Learning: Data Mining, Inference and Prediction*. New York: Springer-Verlag, 2001.

[22] A. F. Kohn and M. F. Vieira, "Optimality in the encoding/decoding relations of motoneurones and muscle units," *BioSystems*, vol. 67, pp. 113–121, 2002.

[23] J. S. Carp, "Physiological properties of primate lumbar motoneurons," *J. Neurophysiol.*, vol. 68, pp. 1121–1132, 1992.

[24] W. S. Smith and E. E. Fetz, "Effects of synchrony between primate corticomotoneuronal cells on post-spike facilitation of muscles and motor units," *Neurosci. Lett.*, vol. 96, pp. 76–81, 1989.

[25] A. Jackson, V. G. J. Gee, S. N. Baker, and R. N. Lemon, "Synchrony between neurons with similar muscle fields in monkey motor cortex," *Neuron*, vol. 38, no. 1, pp. 115–125, 2003.

[26] R. B. Muir and R. N. Lemon, "Corticospinal neurons with a special role in precision grip," *Brain. Res.*, vol. 261, pp. 312–316, 1983.

[27] N. L. Biggs, E. K. Lloyd, and R. J. Wilson, *Graph Theory*. Oxford, U.K.: Clarendon, 1976.

Olivier F. L. Manet is working toward the Ph.D. degree at Université Pierre et Marie Curie, Paris, France.

Marc A. Maier is a Professor at Université Pierre et Marie Curie, Paris, France.